

# Installation Effect on Hover Propeller Performance

Ohad Gur <sup>\*†</sup>, Avi Ayele<sup>\*</sup>, Marek Polčák<sup>\*\*</sup>, Radovan Dítě<sup>\*\*</sup>, and Jan Hubáček<sup>\*\*\*</sup>

<sup>\*</sup> IAI – Israel Aerospace Industries

Lod, 70100-00, Israel

<sup>\*\*</sup> Mejzlik Propellers s.r.o.

Brno-Židenice, 61500, The Czech Republic

<sup>\*\*\*</sup> Energy institute, FME BUT

Brno, 61669, The Czech Republic

[ogur@iai.co.il](mailto:ogur@iai.co.il) - [aavele@iai.co.il](mailto:aavele@iai.co.il) - [polcak@mejzlik.eu](mailto:polcak@mejzlik.eu) - [dite@mejzlik.eu](mailto:dite@mejzlik.eu) - [xhubac10@vutbr.cz](mailto:xhubac10@vutbr.cz)

<sup>†</sup> Corresponding Author

## Abstract

In this paper, the installation effects on hovering air-vehicle performance are discussed. Tractor configuration is considered which exhibits two installation effects on the vehicle performance. The first is the vertical drag due to the immersed installations in the propeller wake. Second is the propeller performance as influenced by the installation wake clogging. An analytic model is suggested for the former and an experiment was done to substantiate an empiric model for the latter. The paper shed light on the procedure of thrust and power bookkeeping, which should be taken into consideration during estimating installed propellers for hovering air vehicles.

## Nomenclature

$A$	=	propeller disk area
$C_{d0}$	=	2-D sectional drag coefficient
$C_D$	=	3-D drag coefficient
$C_P$	=	power coefficient
$C_T$	=	thrust coefficient
$D$	=	propeller diameter
$D_V$	=	vertical drag
$f$	=	equivalent flat plate drag area
$q$	=	dynamic pressure
$S_{ref}$	=	reference area
$v_a$	=	axial induced velocity
$T$	=	thrust
$T_{net}$	=	net thrust
$Z$	=	axial coordinate
$\sigma$	=	solidity
$\rho$	=	density

## Subscripts/Superscripts

$()_{Clogged}$	=	of the clogged condition, with installation effect
$()_{isolated}$	=	of the isolated condition, without installation effect
$()_i$	=	induced

## 1. Introduction

The purpose of this effort is to substantiate a simple, accurate, and validated model of the static operation propeller installation effect.

The model can be used in both test results correction and propeller analysis. This includes:

- a. Predicting the isolated propeller performance from the test rig that includes installation effects
- b. Predicting installation effects of a propeller, knowing its isolated performance
- c. Estimating installation effects of future vehicles

A tractor propeller is probably the most common configuration for hover vehicles – see figs. 1 for the Joby eVTOL UAM (electrical vertical takeoff and landing urban air mobility). Figure 2 shows the Bell-Boeing V-22 Osprey a tilt-rotor configuration is presented. These two vehicles represent the most common hover configuration of using tractor-propellers. For the tractor configuration, the propeller's wake encounters some installations, such as wings and nacelles. These might block or clog the wake path, hence influencing the propeller operation.

Figure 3 shows schematics of a propeller tractor-installation effect. An installation is at a certain distance from the propeller plane, downstream, inside the propeller wake. The propeller wake produces vertical drag on the installation, hence increasing the required thrust of the hovering propeller. In addition, the installation causes a disturbance in the wake, and wake clogging, which influences the conditions on the propeller disk through its induced velocities. This interaction influences the propeller axial induced velocity, its produced thrust, and required shaft power. Hence, the installation effect is considered for both the vertical drag of the installation, and the propeller performance. These two separate influences should be considered for the total thrust/power bookkeeping of the air vehicle.

The separation between the propeller performance and the installation drag is common and is described thoroughly in ESDU 85015 [1]. Note that this ESDU is relevant only for axial flight propellers, hence it is not relevant for hovering propellers.



Figure 1 : Joby Aviation vehicle. URL: <https://www.jobyaviation.com/> [cited October 2022]



Figure 2 : V-22 osprey. URL: <https://news.bellflight.com/> [cited October 2022]

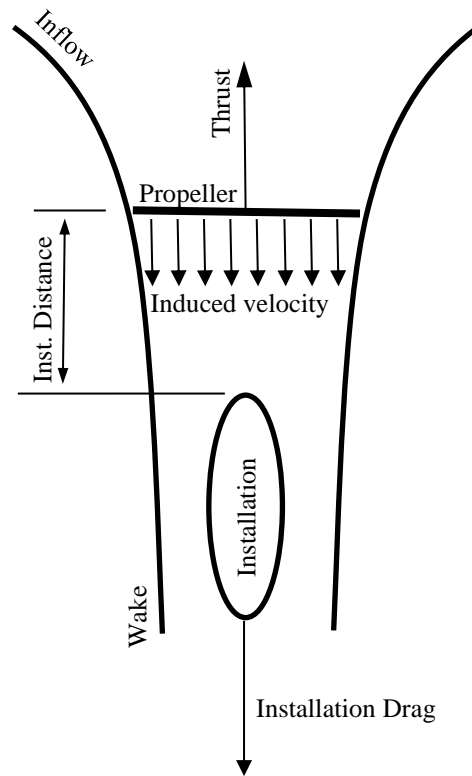


Figure 3 : Hover propeller installation effect

In other cases, no separation is given between the propeller performance and installation drag, which leaves a compound installation effect model. An early example of such a model is given in Diehl's book [2] as depicted in fig. 4. This figure is based on experimental results taken from Fage et al [3] and Weick [4]. The total influence on the propeller efficiency, namely its produced thrust, is given by a factor. This factor depends on the ratio between the body (or installation) diameter and propeller diameter for both pusher and tractor installations. Although it seems crude, it is quite handy in preliminary design efforts.

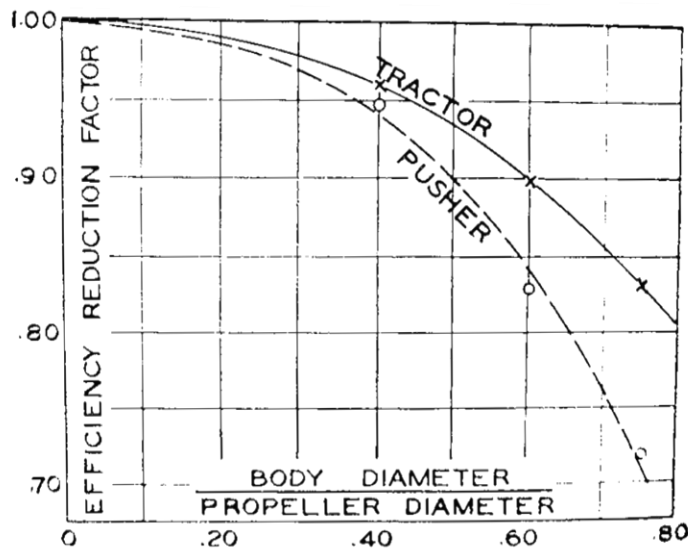


Figure 4 : Body Interference effect on propeller efficiency from Diehl's book [2]

Following this crude model, later Lock and Bateman [5] published a more meticulous method of estimation of the propeller's installation effects. Their method is based on the local change of velocity along the propeller blade, hence the modification of the blade-element model. A similar model is used by Borst [6] to design a new efficient propeller. Harnessing such a model to propeller design is shown by de Gruijl [7].

Using computational fluid dynamics, CFD, many efforts were conducted to find the mutual interaction effect between the propeller and the vehicle. An early analysis using the panel method was done by McCormick et al [8]. Later more accurate CFD analyses were conducted using various methods and techniques such as Euler's equations solver by Dang [9] and Reynolds Average Navier-Stokes, RANS, solvers by Schetz and Favin [10].

Most literature on installation losses concerns axial flight but no static (or hover) operation. These were researched mainly on helicopter rotors and specifically for tail rotors (where the interaction with the vertical fin is substantial). Figure 5 shows a chart that is taken from Prouty's textbook [11] and based on Lynn et al's experiment held in 1970. [12] The same test is used also in Leishman's book [13] to substantiate thrust loss of tail rotor under the influence of a fin. A similar model appears in Keys' report [14] and is shown in fig. 6.

In both figs. 5 and 6, only the net thrust appears, hence both the thrust changes due to interaction together with the fin "drag" due to wake velocity is considered e.g., there is no separation between the two influences.

Comparing the two models in figs. 5 and 6 reveal some differences. While the pusher model is similar, both by values and trends, the tractor configuration, which is more relevant for hovering vehicles, is quite different.

First, in fig. 6 the disk-to-fin gap doesn't influence the interaction, contrary to fig. 5. Second, the influence values in fig. 6 are substantially higher compared to fig. 5.

The reason for such differences is probably due to the lack of tests for a tractor configuration. This might explain the cause of the different "tractor" models which are based on limited data. Note that tractor configuration is less preferable for a helicopter's tail rotor, due to their high interaction losses. This is notable also in Lynn et al [12] test which gives much lower importance to the tractor configuration. This is the reason why most helicopter tail rotors have a pusher configuration; hence the "tractor" configuration is given less attention. This is very different from propellers of hovering vehicles such as tilt rotors and eVTOLs which mostly are tractors.

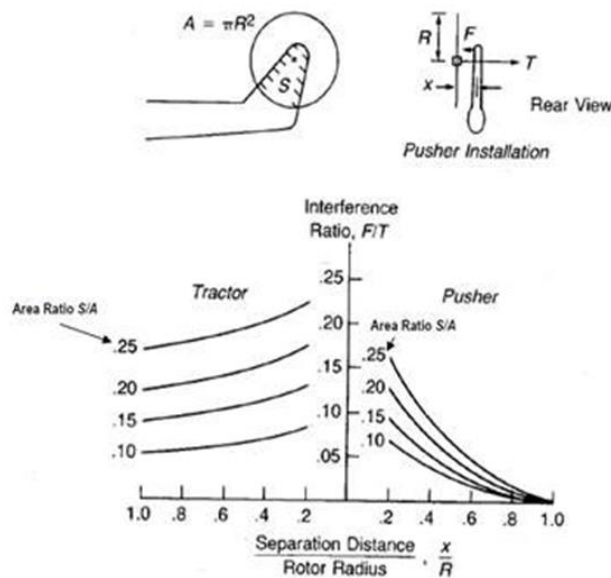


Figure 5 : Tail-rotor/Fin interaction. Taken from Prouty's book [11]

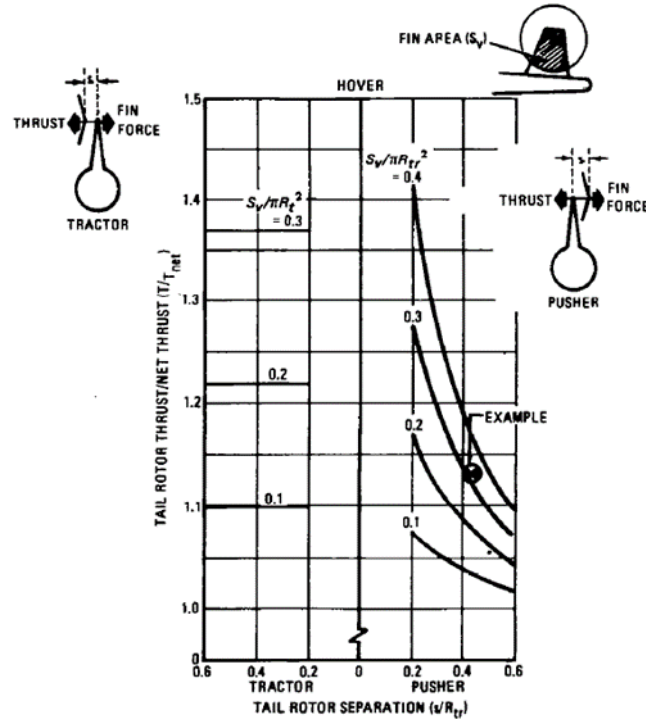


Figure 6 : Tail-rotor/Fin interaction. Taken from Keys' report [14]

In the current effort, using momentum considerations, a simple empiric model is developed. Through normalized installation drag and installation distances, the impact on the propeller thrust and power is found. This can be used later to correct test results or to model propeller installation on future vehicles. In addition, the influence on the vehicle drag bookkeeping is discussed, thus, the total installation effect can be addressed.

The model uses a test campaign held with a series of rotational bodies, immersed in a propeller wake. These have various dimensions and are located at different distances from the propeller disk. A test rig consists of an electric propulsion system covered by an aerodynamic cowling that is used to measure the performance of the various propeller under different installations. By analyzing the test results the influence of the clogging on the propeller performance is found and the general model is substantiated.

## 2. Installation Drag and Thrust Bookkeeping

### 2.1. Installation Drag

The main method for estimating the drag  $D_V$  (sometimes, refers as vertical drag for hovering vehicles) is described in several sources such as Prouty's book [11] in his performance chapter under "vertical drag in hover". A similar method appears in Keys [14] under "fuselage download". In Leishman's book [13] it is mentioned under "vertical drag and download penalty". All these sources deal with the additional drag,  $D_V$ , by summing the drag of various components of the fuselage according to the local wake velocity,  $v_d(z)$ .

In the current case, the vertical drag is defined through an equivalent flat plate drag area,  $f$ . It is the drag force normalized by the dynamic pressure,  $q$ , but it can be described also as the product of the component's drag coefficient,  $C_D$ , by its reference area,  $S_{ref}$ .

$$f = \frac{D_V}{q} = C_D \cdot S_{ref} \quad (1)$$

By that, all installation components, immersed in the propeller wake, share a common reference area.

Knowing the various components (indexed by  $i$ ) equivalent flat plate area,  $f$ , and their location,  $z$ , the drag,  $D_V$ , a calculation is done using simple summation.

$$D_V = \sum_i \frac{1}{2} \cdot \rho \cdot v_a(z_i)^2 \cdot f_i \quad (2)$$

$\rho$  is the air density.

According to ESDU 850151, the induced velocity ratio is a function of the axial distance to propeller diameter ratio,  $z/D$ . This relation also appears in fig. 7.

$$\frac{v_a(z)}{v_a(0)} = f\left(\frac{z}{D}\right) \approx 1 + \frac{1}{\sqrt{1 + \frac{1}{4 \cdot \left(\frac{z}{D}\right)^2}}} \quad (3)$$

Axial momentum theory gives the relation between an isolated propeller's thrust as a measure under isolated conditions (no installation) and axial-induced velocity at  $z = 0$ , on the propeller's disk.

$$v_a(0) = \sqrt{\frac{T_{isolated}}{2 \cdot \rho \cdot A}} \quad (4)$$

Using EQs. (2), (3), and (4) give an estimation for the drag-to-thrust ratio which depends on the installation flat plate areas and installation distances from the propeller disk.

$$\frac{D_V}{T_{isolated}} = \sum_i \frac{1}{4} \cdot \frac{f_i}{A} \cdot \left[ \frac{v_a(z_i)}{v_a(0)} \right]^2 = \sum_i f\left(\frac{f_i}{A}, \frac{z_i}{D}\right) \quad (5)$$

In what follows, the summation and the index  $i$  are omitted for simplicity's sake.

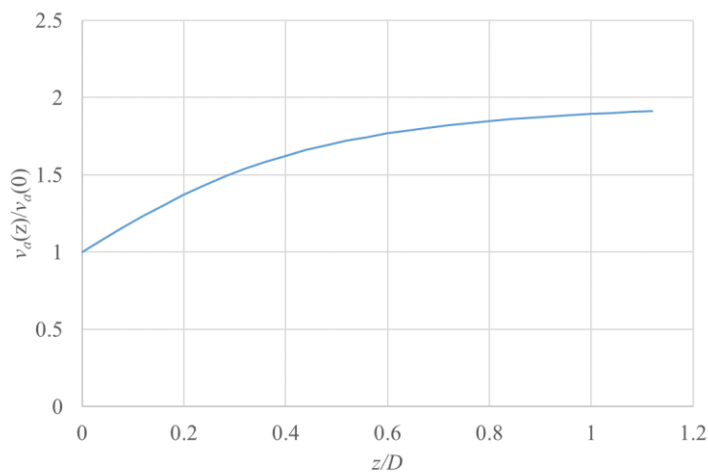


Figure 7 : ESDU 85015 [1] axial induced velocity model as a function of  $z/D$

## 2.2. Power Considerations

The required shaft power can be divided into 2 components: induced power and airfoil-drag power. The following discussion uses the thrust and power coefficient,  $C_T$  and  $C_P$ , respectively.

$$C_T = \frac{T}{\rho \cdot A \cdot V_{tip}^2}; C_P = \frac{P}{\rho \cdot A \cdot V_{tip}^3} \quad (6)$$

where  $\rho$  is the air density,  $A$  is disk area and  $V_{tip}$  is the blade's tip speed.

In the current case hover vehicles are considered, hence the use of EQs. (6) helicopter/rotor normalization is preferred over classic propeller normalization.

Using theoretical blade-element [11],[13] relates between power and thrust coefficient for propeller static operation.

$$C_P = \frac{C_T^{1.5}}{\sqrt{2}} + \frac{\sigma \cdot C_{d0}}{8} \quad (7)$$

where  $\sigma$  is the propeller solidity, and  $C_{d0}$  is the airfoil equivalent drag coefficient.

The first term of eq. (7) is the induced power due to the produced thrust, while the second is the parasite power due to the airfoil drag. Similar to the ground effect, the power which is influenced by the installation is the induced power.[15] Hence the airfoil-drag power coefficient is assumed not to be influenced by the installation merged in the propeller wake.

Equation (7) leads to an empirical relation between the power coefficient,  $C_P$ , proportional to the thrust coefficient by the power of 1.5,  $C_T^{1.5}$ . [16]

$$C_P = A_1 \cdot C_T^{1.5} + A_0 \quad (8)$$

Where  $A_1$  and  $A_0$  are empirical constants. Here  $A_0$  is the required parasite power coefficient (mainly due to the airfoil drag).

## 2.3. Installed Propeller Performance

From the ground effect perspective, both the thrust increase and required-power decrease are the outcome of induced velocity decrease in presence of an obstacle on the wake. The obstacle in the wake influences the induced velocity on the propeller disk, decreasing it, hence for the same thrust, the induced power is decreased.

Also, from momentum consideration, one can assume that the total force on the propeller and the wake should remain similar, hence if the fluid causes drag force on the disturbance, the propeller thrust should increase its thrust, for the same induced power "invested" in the fluid.

Those explanations can relate the thrust of the propeller to the drag,  $D_V$ , of the installation disturbance, or the propeller's required power to the drag-power loss of the disturbance. This brings to the relation between the thrust difference between the clogged and isolated propeller,  $T_{Clogged} - T_{isolated}$ , to the disturbance drag,  $D_V$ . Similarly, the induced power difference,  $P_{i,Clogged} - P_{i,isolated}$ , relates to the power loss of the installation drag.

$$\begin{aligned} T_{Clogged} - T_{isolated} &\propto D_V \\ P_{i,isolated} - P_{i,Clogged} &\propto D_V \cdot v_a(z) \end{aligned} \quad (9)$$

where  $v_a$  is the axial induced velocity that acts on the disturbance, at axial distance  $z$  from the propeller disk.

Normalizing EQs. (9) by  $T_{isolated}$  and using eq. (4) gives normalized parameters for the installation performance effect.

$$\begin{aligned} \frac{T_{\text{Clogged}} - T_{\text{isolated}}}{T_{\text{isolated}}} &\propto \frac{D_V}{T_{\text{isolated}}} \\ \frac{P_{\text{isolated}} - P_{i,\text{Clogged}}}{T_{\text{isolated}} \cdot v_a(0)} &\propto \frac{D_V \cdot v_a(z)}{T_{\text{isolated}} \cdot v_a(0)} \end{aligned} \quad (10)$$

It is assumed that the induced power is equivalent, or relative, to the unclogged, isolated power,  $P_{\text{isolated}}$ . In addition, the vertical drag definition of eq. (2) is substituted in (10)'s righthand side.

$$\begin{aligned} \frac{T_{\text{Clogged}} - T_{\text{isolated}}}{T_{\text{isolated}}} &\approx \frac{T_{\text{Clogged}}}{T_{\text{isolated}}} - 1 \propto \left[ \frac{v_a(z)}{v_a(0)} \right]^2 \cdot \frac{f}{A} \\ \frac{P_{i,\text{isolated}} - P_{i,\text{Clogged}}}{T_{\text{isolated}} \cdot v_a(0)} &\approx 1 - \frac{P_{i,\text{Clogged}}}{P_{i,\text{isolated}}} \propto \left[ \frac{v_a(z)}{v_a(0)} \right]^3 \cdot \frac{f}{A} \end{aligned} \quad (11)$$

Hence the two parameters on which the installation effect depends are  $f/A$  and  $z/D$ .

$$\begin{aligned} \frac{T_{\text{Clogged}}}{T_{\text{isolated}}} - 1 &= f_1 \left( \frac{z}{D}, \frac{f}{A} \right) \\ 1 - \frac{P_{i,\text{Clogged}}}{P_{i,\text{isolated}}} &= f_2 \left( \frac{z}{D}, \frac{f}{A} \right) \end{aligned} \quad (12)$$

Using the test campaign,  $f_1$  and  $f_2$  empiric models are found and discussed thoroughly in the following paragraphs. It is assumed that for thrust/power bookkeeping, both  $f_1$  and  $f_2$  are known with a reasonable level of confidence.

## 2.4. Thrust/Power Bookkeeping

For a propeller installed at a tractor configuration, the net thrust,  $T_{\text{net}}$ , is the outcome of the thrust bookkeeping. This is the thrust that is used to elevate the vehicle during hover, hence it equals the vehicle's weight at steady hovering. This thrust,  $T_{\text{net}}$ , is the sum of the propeller thrust under the installation effect and the vertical drag,  $D_V$ . Here the produced propeller thrust under installation effect is referred to as the "clogged" thrust,  $T_{\text{clogged}}$ . This is contrary to an uninstalled propeller, operating under isolated conditions, hence  $T_{\text{isolated}}$ .

Note that the propeller installed thrust,  $T_{\text{clogged}}$ , and the installation drag,  $D_V$ , act in an opposite direction. This bookkeeping results in the relation between the isolated propeller thrust and the two components of the thrust bookkeeping.

$$T_{\text{net}} = T_{\text{clogged}} - D_V = T_{\text{isolated}} \cdot \left( \frac{T_{\text{clogged}}}{T_{\text{isolated}}} - \frac{D_V}{T_{\text{isolated}}} \right) \quad (13)$$

The first term in the parenthesis is the clogged-to-isolated thrust ratio. This model is substantiated in the following paragraphs using a test campaign. The second term in the parenthesis is the vertical drag to isolate-thrust ratio, as found in eq. (5). It is a function of both  $f/A$  and  $z/D$ .

In a practical case of thrust bookkeeping for a hovering vehicle, the isolated propeller performance data is given by the propeller manufacturer. This means that the isolated propeller data is given, and its installed performance under the required thrust is estimated.

The following parameters are required to estimate the required power of this installed propeller on a given air vehicle:

- a.  $C_{T\text{-isolated}}$  and  $C_{P\text{-isolated}}$ , - isolated propeller thrust and power coefficients. In most cases, these characteristics are given by the propeller manufacturer or through analyses.
- a.  $f/A$  – estimation of the equivalent-flat-plate-area of the installation components, immersed in the propeller's wake
- b.  $z/D$  – the position of these components

- c.  $T_{net}$  – the required net thrust at the end of the bookkeeping. In most cases, it is a requirement based on the vehicle weight and additional measures of conservative e.g., control margin.
- d. Operating conditions:  $\rho$  and propeller speed ( $V_{tip}$ ).  
It is assumed that the propeller speed is the same for the isolated and clogged operation. This enables finding  $V_{tip}$  from the isolated propeller performance,  $C_{T,isolated}$  vs.  $C_{P,isolated}$  as if  $T_{net}$  is equal to  $T_{isolated}$ . Otherwise, some iterations are required which influence the final results in a negligible manner.

The calculation of the required power for the net thrust,  $T_{net}$ , is done according to the following steps.

- a. Using the clogging model of EQs. (12) finding  $T_{clogged}/T_{isolated}$
- b. Using eq. (5)  $Dv/T_{isolated}$  is found
- c. Using eq. (13)  $T_{isolated}$  is found
- d. Calculating  $T_{clogged}$  and normalizing it to  $C_{T,clogged}$

$$C_{T,clogged} = T_{isolated} \frac{T_{clogged}/T_{isolated}}{\rho \cdot A \cdot V_{tip}^2} \quad (14)$$

- e. Using  $A_1$  and  $C_{T,clogged}$ , finding  $P_{i,isolated}$ , for the required operating conditions

$$P_{i,isolated} = \left( A_1 \cdot C_{T,clogged}^{1.5} \right) \cdot \rho \cdot A \cdot V_{tip}^3 \quad (15)$$

- f. Using the clogging model of EQs. (12) finding  $P_{i,clogged}/P_{i,isolated}$  and from it finding  $P_{i,clogged}$
- g. Finding  $P_{clogged}$  by adding the parasite power, based on  $A_0$

$$P_{clogged} = P_{i,clogged} + A_0 \cdot \rho \cdot A \cdot V_{tip}^3 \quad (16)$$

Note that the reverse procedure is also available. This is important mainly for propeller manufacturers which like to substantiate the isolated propeller performance out of test rigs or flight test results.

### 3. Propeller Performance Installation Effect Model

One of the main gaps in the model is the functions  $f_1$  and  $f_2$  in EQs. (12). These are empirical models which result from test campaign. In what follows such a campaign is described in detail, as conducted in the Mejzlik facility.

#### 3.1. Test Procedure

The test campaign was held by Mejzlik Propellers s.r.o. in their facility. The propellers are installed on a dedicated test rig which enables the measurement of the produced thrust, engine torque, and engine speed. Note that for the current effort the electric system measurements (current and voltage) aren't relevant. The rig and the installation are depicted in fig. 8. The basic measurement system is constructed of an aerodynamic-shaped nacelle which capsules the electric propulsion system as shown in fig. 9.

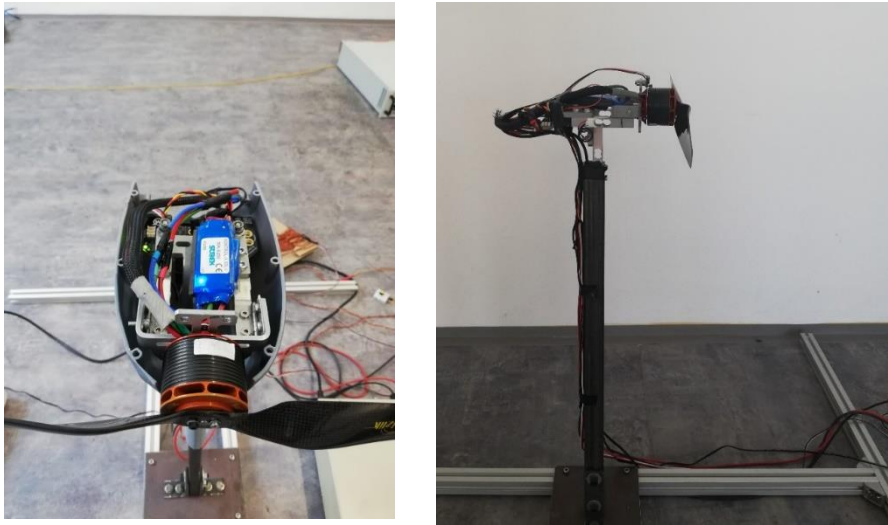


Figure 8 : Test rig and propulsion system buildup



Figure 9 : The test rig, with and w/o fairing

To simulate the clogging effect, several rings were installed on the nacelle at two positions: forward and aft. figure 10 depicts these two positions. Z1 stands for the forward position (Z1~80 mm) and Z2~210 mm is the aft position. Figure 11 shows the installation of the clogging ring at its forward position together with an 18x6 propeller. 3 ring sizes are used according to their external diameter: 9, 12.7, 15.6, and 18-inch diameter. These represent clogging of 25%, 50%, 75%, and 100%, of an 18-inch diameter disk, respectively.

Four different propellers are tested: 18x6, 20x6.7, 16x5.7, and 22x7.4. All are 2-bladed, designed, and produced by Mejzlik Propellers. By testing different diameter propellers, various  $z/D$  and  $f/A$  are covered, hence wide database is substantiated.

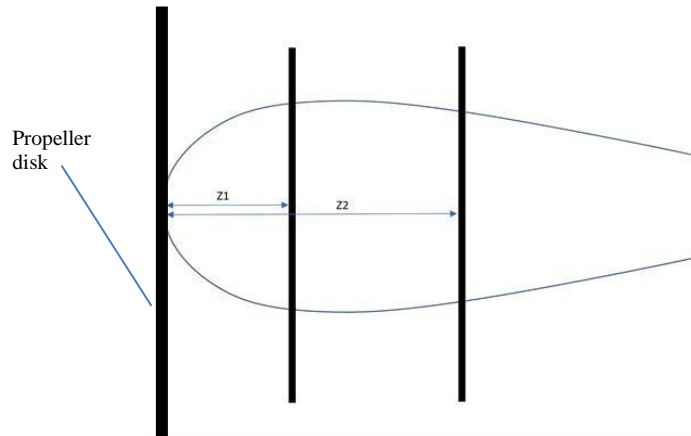


Figure 10 : Clogging ring axial position



Figure 11 : Installation of forward, 25% clogging ring with 18x6 propeller

### 3.2. Drag Analysis

CFD analysis was conducted for nacelle with various ring configurations under homogeneous airspeed, without the influence of the propeller. The analysis was conducted for airspeeds of 15 and 20 m/sec @S.L., standard atmosphere. EZair RANS software was used with SST  $k-\omega$ , 2<sup>nd</sup> order turbulent model. Adequate residuals convergence was reached. Figure 12 shows pressure distribution for 2 representative cases: an isolated nacelle and an 18" diameter ring.

The resulting drag was normalized by the freestream dynamic pressure,  $q$ , hence the equivalent-flat-plate-area,  $f$ , was found as defined in eq. (1). The equivalent flat plate area is presented in fig. 13 as a function of the clogging ratio (relative to 18" diameter).

The “no ring” data exhibited negligible drag area, hence the “isolated” propeller’s performance is considered as the “no-ring” configuration, without clogging rings. Although the nacelle has some influence, it is considered to be fairly aerodynamic, minimizing the propeller installation effects.

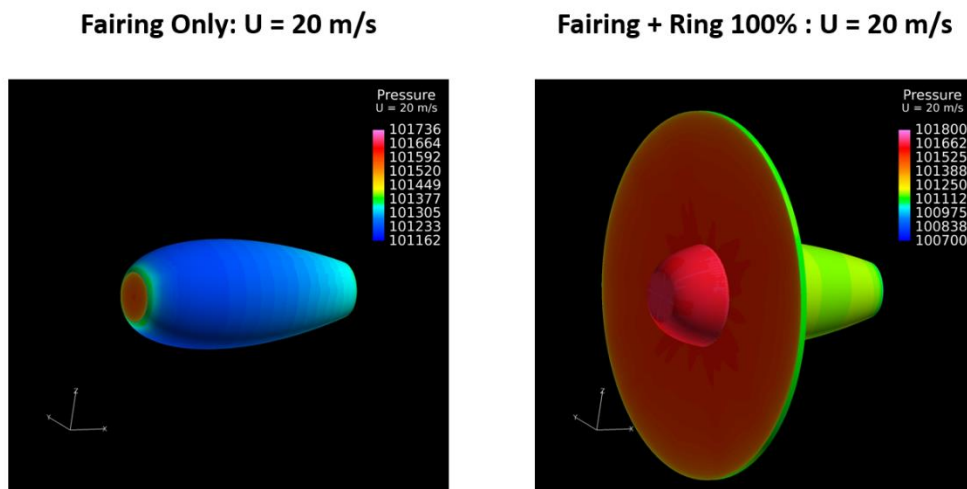


Figure 12 : CFD results, pressure distribution for clean nacelle, and 100% ring

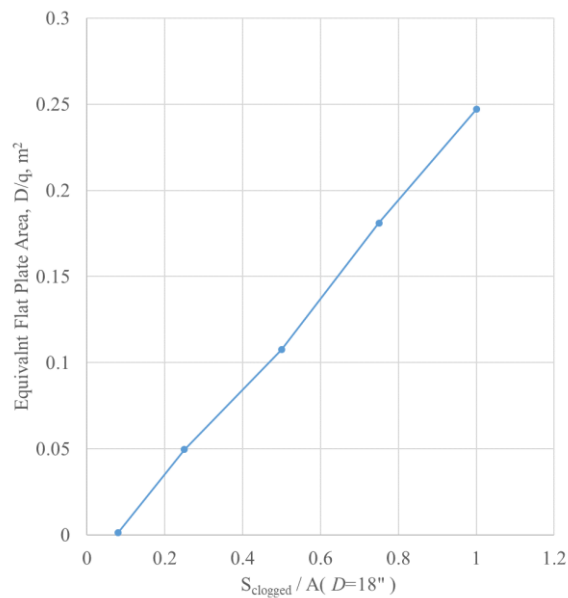


Figure 13 : CFD results, EFPA vs clogging area ratio

### 3.3. Test Results and Model Substantiation

The thrust and power test results were normalized by the “isolated”, non-clogging results. Hence the parameters  $T_{clogged} / T_{isolate} - 1$  and  $1 - P_{i,clogged} / P_{i,isolated}$  are found for various  $z/D$  and  $f/A$ . Figure 14 exhibits all test point scattered as a function of  $f/A$ , with a color scheme relates to the various  $z/D$  parameters. The test points exhibit a clear trend and curves are fitted through the average values of these test points.

The results' trends are clear and definite. As the drag area ratio,  $f/A$ , increases, the impact on the propeller performance is more substantial. This is true also as the installation distance ratio,  $z/D$  decreases.

For these cases (proximity to the disk and high drag area ratio) the thrust increase by up to 20% above its net value, and induced power decreases by up to 40%.

These are all effects that can be related to pseudo-ground-effect. For ground effect, only the ground proximity (namely  $z/D$ ) is relevant as shown in Hayden's paper [15] but for partial blockage of the wake, the dependency on the drag-area ratio,  $f/A$  is not trivial.

The induced-power chart exhibits some anomalies. For example, the  $z/D=0.197$  curve seems too low compared to  $z/D=0.175$ . In addition, the  $z/D=0.517$  curve exhibits negative values. The induced-power curves exhibit lower accuracy which relates to the substantiation of the induced power out of the measured shaft power. As shown in EQs. (8), the induced power is a part of the total shaft power, and substantiating it requires some empirical assumptions and introduces inaccuracies.

Using the data presented in fig. 14, two models were substantiated for the thrust and power installation effects, based on EQs. (12).

$$\begin{aligned} \frac{T_{Clogged}}{T_{isolated}} - 1 &= f_3 \left( \frac{z}{D} \right) \cdot \left( \frac{2}{1 + e^{-2.5 \cdot \frac{f}{A}}} - 1 \right) \\ f_3 \left( \frac{z}{D} \right) &= \begin{cases} -3.0 \cdot \frac{z}{D} + 0.62 & \frac{z}{D} < 0.16 \\ -0.3673 \cdot \frac{z}{D} + 0.1975 & 0.16 \leq \frac{z}{D} \leq 0.538 \\ 0 & \frac{z}{D} > 0.538 \end{cases} \\ 1 - \frac{P_{i,Clogged}}{P_{i,isolated}} &= f_4 \left( \frac{z}{D} \right) \cdot \left( \frac{1}{1 + \frac{0.15}{(f/A)^{2.3}}} \right) \\ f_4 \left( \frac{z}{D} \right) &= \begin{cases} -12.6943 \cdot \frac{z}{D} + 2.493264 & \frac{z}{D} < 0.175 \\ -0.7709405 \cdot \frac{z}{D} + 0.3845944 & 0.175 \leq \frac{z}{D} \leq 0.5 \\ 0 & \frac{z}{D} > 0.5 \end{cases} \end{aligned} \quad (17)$$

Figure 15 shows the empiric models versus test results (via its average curves). The model fits well the test data and captures in a good manner the influence of both  $z/D$  and  $f/A$ .

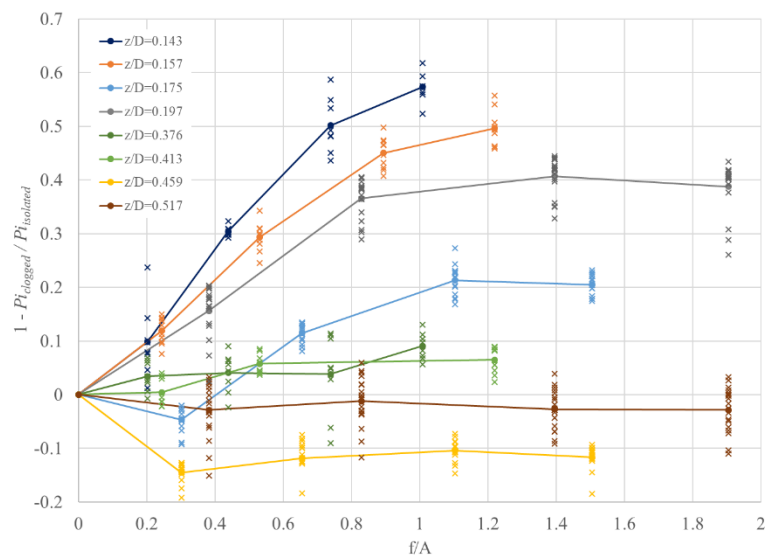
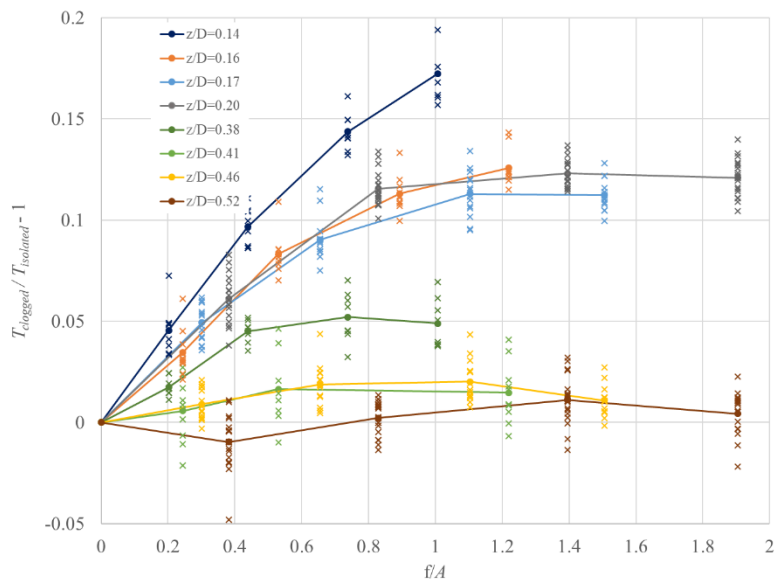


Figure 14 : Dependency of propeller thrust and induced power on  $z/D$  and  $f/A$

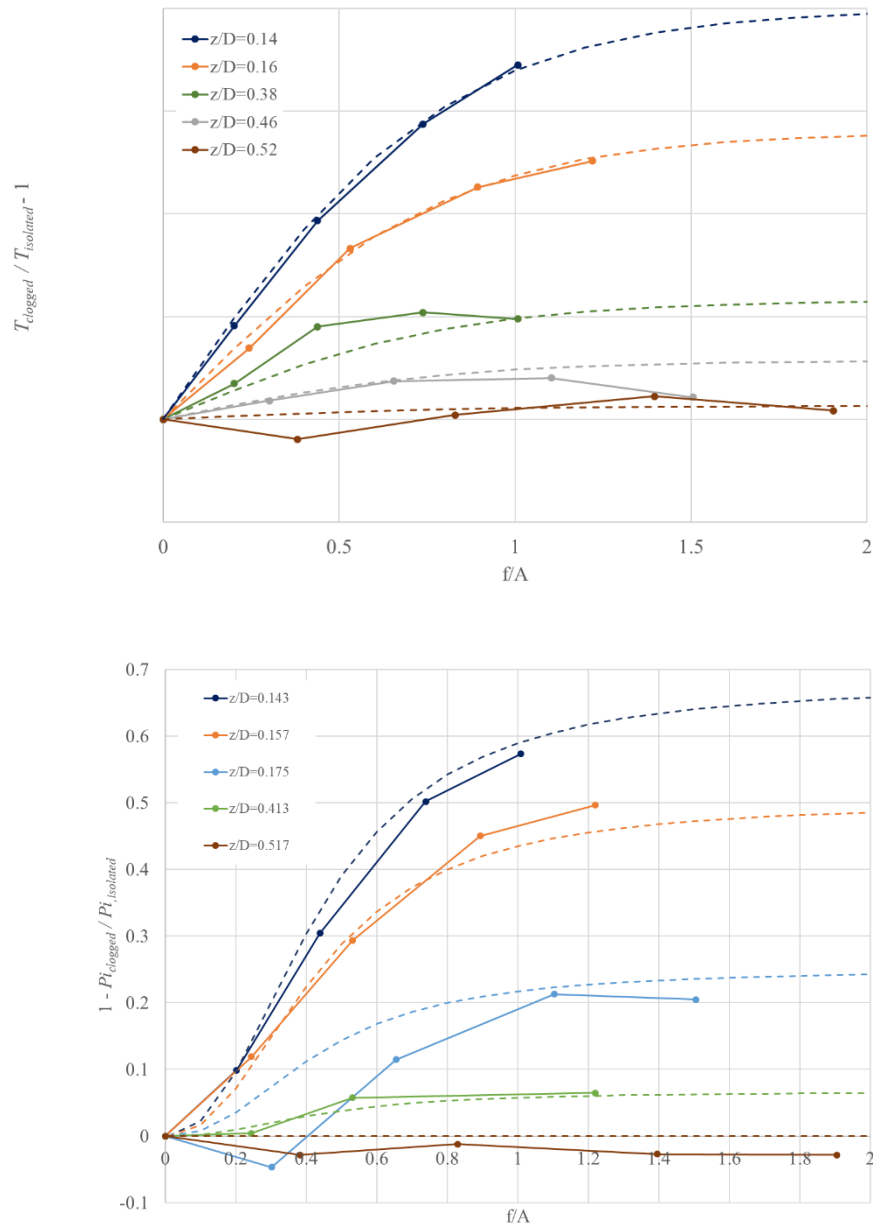


Figure 15 : Thrust and power clogging models vs. test results

### 3.4. Installation Model Validation

To validate the suggested model, an additional test campaign was conducted, this time with a clogging obstacle that is "half ring" shaped.

This enables some limited validation of the model for non-axisymmetric cases and different  $f/A$  values.

On these tests, both full and half rings were used and the data were analyzed in the same manner as shown above. A single propeller, Mejlzik 18x6 is used with  $z/D=0.18$ . the results are presented in fig. 16. For the thrust effect, the model exhibits good accuracy, while the induced power is somewhat less accurate, although grasping the trends in a good manner. As shown above, the induced-power model is less accurate, although it gives a good approximation to test results.

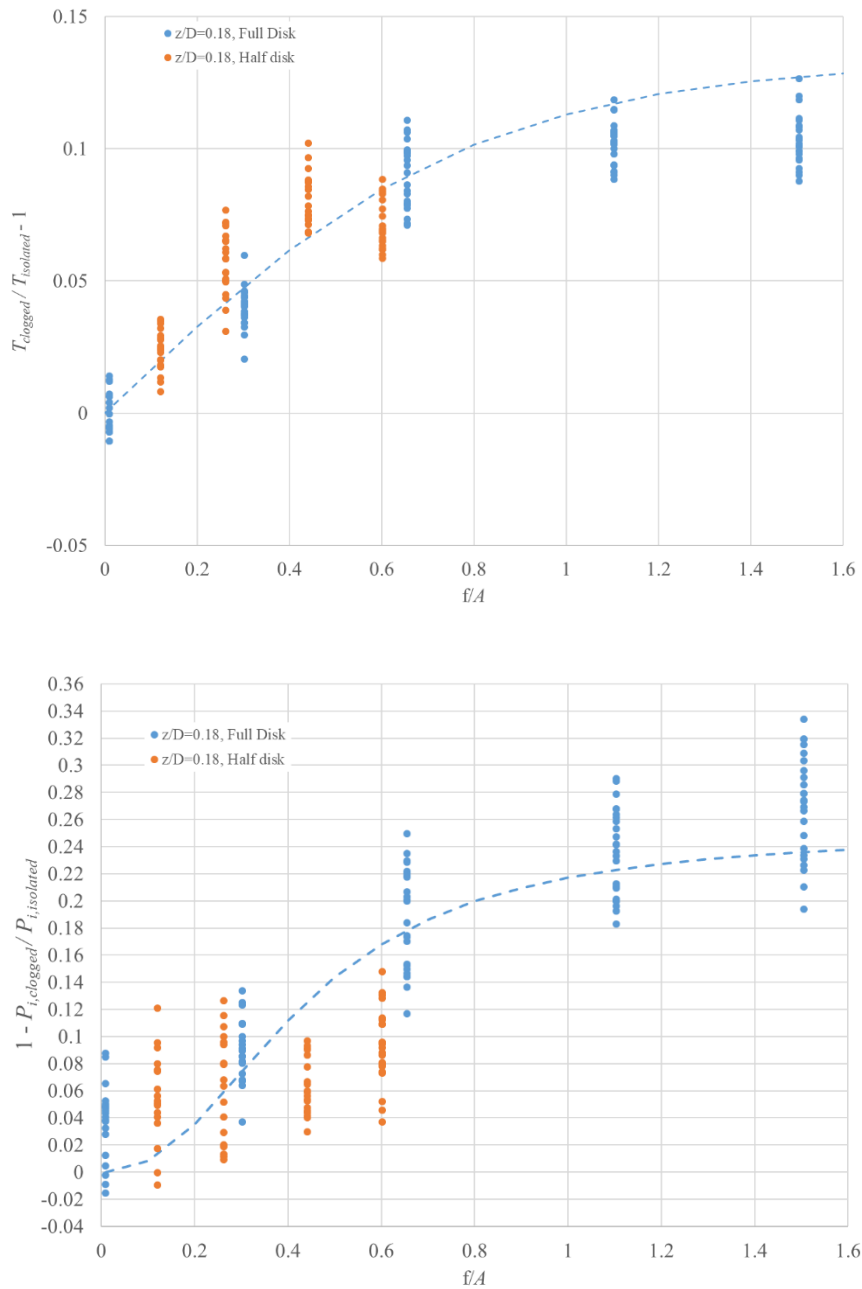


Figure 16 : Full and half ring clogging experiments

## 4. Summary and Conclusions

The paper describes the thrust and power influence on a hover propeller due to installation immersed in its wake. For many hovering air vehicles, a tractor propeller is installed above the vehicle, while all its supports, engines, etc. are located below the propeller disk. These components interact with the propeller wake/down-wash and affect the propeller performance. The propeller wake interacts with these components and produces vertical drag, which increases the required total thrust of the propeller. Understanding the interaction between the installation and the propeller is required for reliable performance estimation of the entire air vehicle.

Through simple momentum consideration, these interactions are modeled, providing thrust and power bookkeeping procedures. The suggested method requires mainly the non-installed/isolated propeller performance which in most cases is given by the propeller manufacturer. In other cases, this isolated performance can be estimated through analysis. In addition, the model requires the drag area of the installation immersed in the propeller wake and its axial position - the distance between the installation and the propeller disk. By these parameters, one can estimate the required power by the propeller which produces the specified required net thrust.

The suggested model enables estimating the installation influence in a relatively simple way. The main gaps to complete in the bookkeeping procedure are the propeller thrust and induced-power isolated-to-installed ratios. These two ratios are a function of two non-dimensional parameters: drag-area to disk-area and installation-distance to propeller-diameter ratio.

Using a test campaign, the two required isolated-to-installed ratios (power and thrust) are found and an empiric model is substantiated. The experiments use both an isolated propeller and a set of axisymmetric disks, positioned in various locations behind the propeller. The empirical model was substantiated by testing a range of propeller diameters, ring sizes, and installation locations. After normalizing all data, the data exhibits specific trends which enable, through curve fitting, an empirical model. Using this model allows us to conduct the full thrust/power bookkeeping, enabling a relatively simple estimation of the installation effect.

The empiric model exhibits a good comparison to the thrust isolate-to-clogged ratio. For the induced-power model, the comparison is less accurate although the trends are captured in a good manner. Induced power cannot be measured directly and has to be estimated. The induced power is calculated by subtracting an estimated parasite power (due to cross-sectional drag) from the measured shaft power. This causes some degradation in the accuracy of the results. Still, the resulting model is practical and gives reasonable estimations.

To demonstrate the model's correctness, test validation was conducted using a separate test campaign. This additional test uses non-axisymmetric disks, rather than the axisymmetric disks, which were used in the main campaign. By installing non-axisymmetric obstacles in the propeller wake, the measured thrust and power can be compared to the suggested model using the same parameters. After simple processing, the test results exhibit a good comparison to the empiric model. This proves that the model can be used for general installation, rather than axisymmetric disturbances. In the non-axisymmetric installation, the thrust behavior exhibits better agreement with the model while the induced power is captured less accurately. This repeats the basic empiric model accuracy trend - better agreement of the thrust compared to the induced-power model.

The presented installation effect estimation is very practical. With few parameters concerning the isolated propeller and the installation properties, one can evaluate at a good accuracy the propeller installed performance. This can be used not only for small-scale propellers but also for other scales with the relevant normalized parameters. Moreover, the suggested procedure can be improved by additional test data, hence improving the empirical model's correctness.

## References

- [1] The Royal Aeronautical Society, "Introduction to installation effects on thrust and drag for propeller-driven aircraft," ESDU 85015, August 2006.
- [2] Diehl W.S., "Engineering aerodynamics," The Ronald Press Company New York, 2nd Ed., 1936.
- [3] Fage A. Lock C.N.H., Bateman H., and Williams D.H., "Experiments with a family of airscrews including the effect on tractor and pusher bodies, Part II—Experiments on Airscrews with Tractor and Pusher Bodies" Aeronautical Research Committee Research & Memoranda No. 830, November 1922.
- [4] Weick, F.E., "Full-Scale Wind Tunnel Tests with a Series of Propellers of Different Diameters on a Single Fuselage," NACA Report 339, 1931.
- [5] Lock C.N.H. and Bateman H., "Interference between bodies and airscrews," Aeronautical Research Committee Research & Memoranda No. 1445, June 1931.
- [6] Borst H.V., "Propeller performance and design influenced by the installation," SAE 810602, Society of Automotive Engineers, Business Aircraft Meeting & Exposition, 7th-10th April 1981, Wichita Kansas.
- [7] de Gruijl W, "The impact of installation effects on propeller design optimization for aerodynamic and aeroacoustic performance," MSc Thesis, Delft University of Technology, May 2022.

- [8] McCormick B.W., Aljabri A.S., Jumper S.J., and Martinovic Z.N., "The analysis of propellers including interaction effects," SAE 790576, Society of Automotive Engineers, Business Aircraft Meeting & Exposition Century II, 3rd-6th April 1979, Wichita Kansas.
- [9] Dang T.Q., "Simulations of propeller/airframe interference effects using an Euler correction method," *Journal of Aircraft* Vol. 26 No. 11, 1989, pp. 994-1001.
- [10] Schetz J.A. and Favin S., "Numerical solution of a body-propeller combination flow including swirl and comparison with data," AIAA Paper 79-4056, *Journal of Hyrdonautics*, Vol. 13, No. 2, 1979, pp. 46-51.
- [11] Prouty R.W., *Helicopter performance, stability, and control*, PWS Publishers Boston, 1986.
- [12] Lynn R.R., Robinson F.D., Batra N.N., and Duhon J.M., "Tail rotor design, Part I: Aerodynamics," *Journal of the American Helicopter Society*, Vol. 15, (4), 1970, pp. 2-15.
- [13] Leishman J.G., "Principles of helicopter aerodynamics," Cambridge University Press, Cambridge Aerospace Series, 2nd Edition, 2006.
- [14] Keys C.N., "Rotary wing aerodynamic, vol II – performance prediction of helicopters," NASA CR-3083, January 1979.
- [15] Hayden J.S., "The effect of the ground on helicopter hovering power required," 32nd Annual National V/STOL Forum of the American Helicopter Society, 10-12 May 1976, Washington DC.
- [16] Picasso B. D., Buckanin R.M., Downs G.T., and Herbst M.K., "Airworthiness and flight characteristics (A&FC) test of YAH-64 advance attack helicopter, prototype qualification test-government (PQT-G), part 3 and production validation test - government (PVT-G) for handbook verification," USAAEFA PROJECT NO. 80-17-3, October 1982.